Narrow Bandpass Filters Using Dual-Behavior Resonators

Cedric Quendo, Eric Rius, and Christian Person

***Abstract*—This paper reports on a new concept of narrow bandpass filters leading to perfectly controlled electrical responses within both the required operating bandwidth and adjacent undesired bands. A specific topology is considered for such a "global synthesis": in comparison with conventional filter performances, it provides significant improvements in terms of rejection control. The attenuated frequencies are each located apart from the bandpass frequencies and controlled by means of n transmission zeros introduced through original dual-behavior resonators (DBRs). These resonators are based on the association of different parallel open-ended stubs and allow the designer to independently control the in-band and out-of-band responses of the filter. A global synthesis approach is also discussed on a simplified architecture based on stepped impedance stubs, and the experimental results shown clearly validate the proposed concept. This simplification reduces the number of degrees of freedom when designing a DBR, and consequently the two transmission zeros become dependent.**

***Index Terms*—Filter synthesis, microstrip technology, microwave bandpass filter, open-ended stubs.**

I. Introduction

THE expansion of new telecommunication systems has brought severe constraints and particular requirements for RF front-ends and especially for RF filters [1]. Electrical performances regarding either out-of-band rejection or in-band transmission losses as well as cost, reliability, or dimensions have to be considered. For example, RF filters are commonly used inside receivers with drastic specifications about rejection in the adjacent transmitted frequency band to preserve them from possible damage and degradations due to high TX power. High-order filters are, therefore, required with classical topologies, but, unfortunately, they lead to high insertion losses and a significant degradation of the carrier-to-noise ratio (CNR). These difficult problems are studied intensively in microwave filters. These studies are based on technology, on the one hand [2], [3], and on specific investigations that are being made about new filter topologies including transmission zeros, on the other hand.

The use of multimode resonators for waveguide application or dielectric resonators seems to be a good solution [4]–[10] but it presents several problems such as weight, cost, tuning, and sensitivity. In this way, planar filters present a great interest, but they are not as efficient as waveguide filters in terms of losses.

Manuscript received November 14, 2001; revised October 21, 2002.

The authors are with the Laboratoire d'Electronique et des Systèmes de Télécommunication, BP 809, 29285 Brest, France (e-mail: eric.rius@univ-brest.fr).

Digital Object Identifier 10.1109/TMTT.2003.808729

Some planar applications have been inspired by waveguide methods using dual-mode ring resonators, but they are complex to design [11]–[13].

For planar applications, some of this work involves modifying the lumped scheme and using Richards' transformations. This solution is very interesting, but does not really use the intrinsic specificity of distributed elements due to the utilization of equal length or commensurate transmission lines [14]–[21].

Malherbe [22] demonstrated that it was possible to realize more efficient filters by using noncommensurate transmission lines [23], [24]. Later, Salerno *et al.* [25] went beyond these considerations and made an interesting statement about the design of microwave filters. Their conclusion was that it is desirable to adopt a design procedure operating directly on the microwave structure. Indeed, in this way, some degrees of freedom can be used to improve the performances of filters.

These last few years, some topologies have been developed by considering this philosophy [26]–[29].

In this paper, we also adopt this philosophy to design new resonators and develop a topology of filters which allows the independent control of the rejected bands by adding transmission zeros as well as the centered bandpass. To design such specific filters, we investigated basic resonators that show a dual-frequency behavior in the bandpass and in the stopband regions [30]. However, the quarter-wavelength inverters are preserved in order to allow the application of the slope parameter method, and thus to develop an exact, general and analytical synthesis.

Such dual-behavior resonators (DBRs) are realized by associating two different parallel open-ended stubs. Each stub brings its own transmission zero depending on its fundamental resonant condition. At the same time, this original association can be transparent within a given operating frequency bandwidth once the stubs have been properly connected under constructive recombination criteria. This will result in a bandpass response created between the above-mentioned lower and upper rejected bands.

According to the number of available parameters and the initial behavior of each stub, this DBR allows an independent control of each interesting frequency band of the response, i.e., the center frequency bandpass and the attenuated bands. The frequency response of an nth-order filter (composed of n fundamental resonators) presents the following:

- n poles in the operating bandwidth;
- n transmission zeros in the lower attenuated band;
- n transmission zeros in the upper attenuated band.

In Section II, we will develop the basic equations relating to this generic structure in order to propose a practical syn-

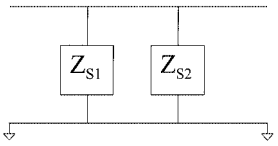

Fig. 1. DBR: the basic resonant structure.

thesis for designing the filter. The synthesis will establish a correspondence between the physical parameters of the resonators (characteristic impedances, lengths, and geometrical segmentation) and the electric characteristics of the ideal filter (central frequency, bandwidth, and transmission zeros).

Depending on the number of variables and the numerical difficulties for solving these analytical equations, simplifications can then be proposed and lead to an easier and practical synthesis procedure. These simplifications imply a frequency dependence of the two transmission zeros associated with each elementary resonator and, then, impose constraints on the electrical response. This is discussed in Section III.

Nevertheless, despite the number of variables—or tuning parameters—that is consequently decreased, the numerous possibilities still presented by the structures can be used efficiently. This is illustrated via different examples corresponding to a second-order filter. Finally, experimental validations of the proposed concept are given by means of a microstrip technology implementation.

II. Basic Idea: The DBR

The generic structure (see Fig. 1) can be described as a parallel association of two different bandstop structures of equivalent input impedances Z_{s1} and Z_{s2}. Obviously, the impedance of the whole structure is defined as

$$Z = \frac{Z_{S1} Z_{S2}}{Z_{S1} + Z_{S2}}. \tag{1}$$

This equation shows that the stub association has no incidence on the frequencies of the transmission zeros that always appear when $Z = 0$, i.e., when $Z_{s1} = 0$ or $Z_{s2} = 0$. The individual incidence of each bandstop structure is then preserved. Nevertheless, a bandpass can be created when the equivalent input impedances Z_{s1} and Z_{s2} have the same modulus, but become out-of-phase. Indeed, in this case, the total impedance Z tends toward infinity.

The electrical response of a classical open-ended stub connected to a 50-Ω transmission line is presented in Fig. 2 over a wide frequency range. The transmission zeros of such a structure appear at frequencies for which the length L of the stub corresponds to an odd multiple of $\lambda_0/4$ ($L = (2k+1)\lambda_0/4$), assuming a propagation medium equivalent to air. A geometrical decomposition of this stub into two cascaded transmission lines with different characteristic impedances may be considered in order to modify such a transmission zero location. This can be done with or without changing the overall stub length.

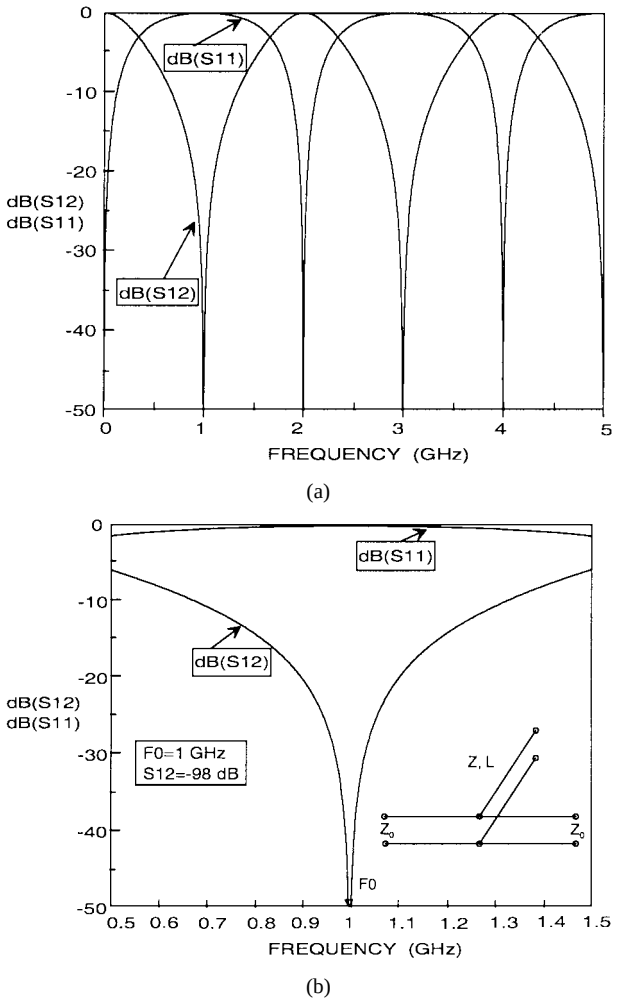

Fig. 2. Electrical response of a classical open-ended stub. (a) Broad-band frequency response. (b) Zoom-in for narrow-band characteristics.

Here, we focus on the first transmission zero control (see Fig. 2) for which the frequency shift can be positive or negative according to the impedance ratio Γ

$$\Gamma = \frac{Z_{\text{first section line}}}{Z_{\text{second section line}}} \tag{2}$$

where $Z_{\text{first section line}}$ and $Z_{\text{second section line}}$ are the characteristic impedances of the stub transmission line sections located near the Tee-junction and the open-ended extremity, respectively.

If $\Gamma < 1 (\Gamma' > 1)$, then the frequency associated with the transmission zero increases (decreases) as illustrated in Fig. 3. (Fig. 4). These two basic resonant structures can be connected in parallel. The different characteristic impedance values as well as their equivalent electrical lengths can be adjusted so as to ensure a constructive recombination at a given frequency F_o. In the two examples presented here, the lengths l of the different section lines were chosen equal to $L/2$, where L is the length of the corresponding uniform stub whose response is presented in Fig. 2.

As depicted in Fig. 5, the structure is equivalent to a bandpass filter at F_o, whereas transmission zeros still have an independent behavior on each side of the bandpass. The number of variables

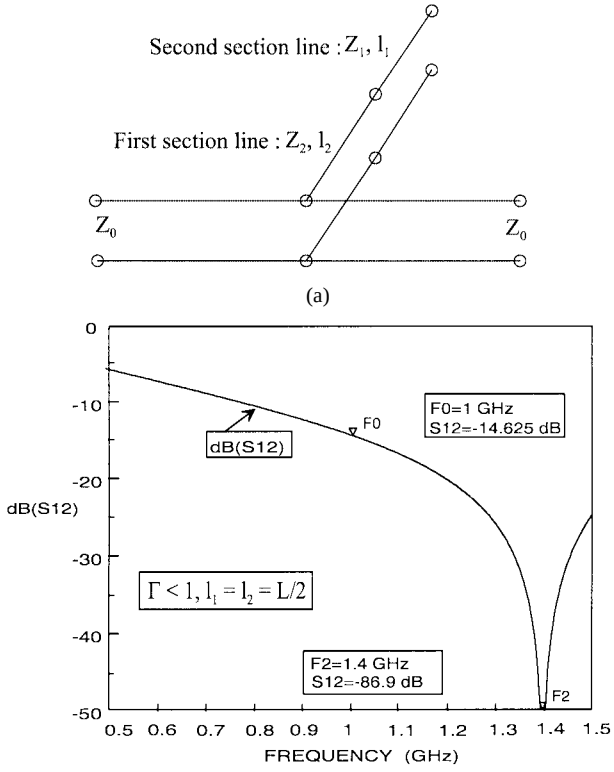

Fig. 3. Stepped impedance stub with $\Gamma < 1$. (a) Ideal transmission-line scheme. (b) Electrical response.

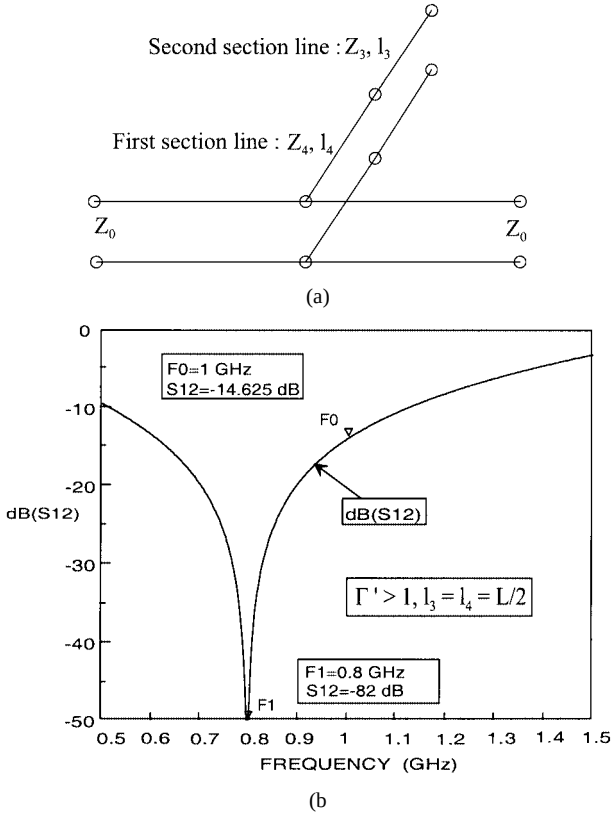

Fig. 4. Stepped impedance stub with $\Gamma' > 1$. (a) Ideal transmission-line scheme. (b) Electrical response.

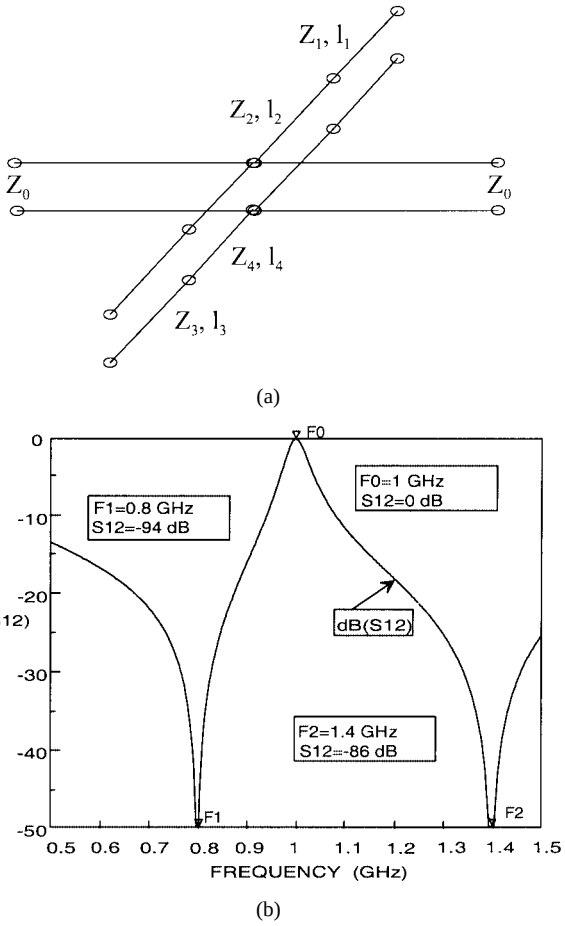

Fig. 5. DBR structure. (a) Ideal transmission-line scheme. (b) Electrical response.

available here (characteristic impedances Z_1, Z_2, Z_3, and Z_4 and electrical lengths l_1, l_2, l_3, and l_4) can be used efficiently for controlling independently the center frequency F_o and the transmission zero frequencies, i.e., the out-of-band rejections, in accordance with (1).

This structure can, therefore, be considered as the generic element of a new class of bandpass filters with improved out-of-band response. For an nth order bandpass filter (nth DBRs), n poles are obtained within the operating bandwidth, whereas n transmission zeros can be independently placed in the lower undesired frequency band as well as in the upper one.

The electrical principles now being well established, we implemented suitable analytical formulations to identifying the physical parameters of this new topology with the filter basic electrical specifications.

III. Synthesis

A. General Formulation

As shown above, for an nth-order filter, a given transmission zero is clearly related to one of its $2n$ constituting stubs, i.e., one of the n DBRs. Its location can be calculated by considering the equivalent input impedances Z_{S1} and Z_{S2} of these stubs for one DBR (see Fig. 6).

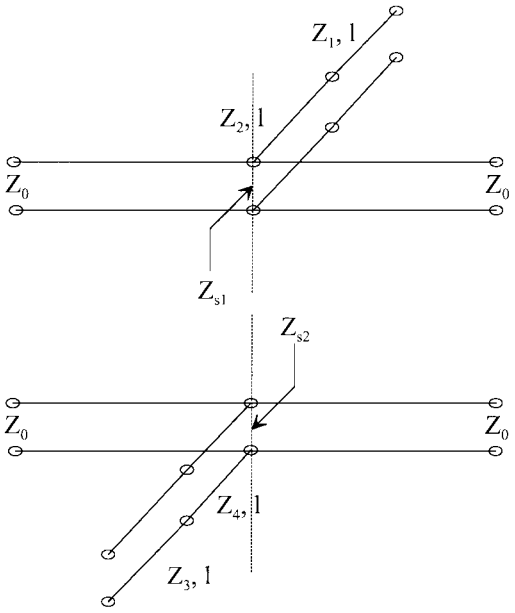

Fig. 6. Equivalent input impedances Z_{s1} and Z_{s2}.

In order to simplify future expressions, the lengths of the section lines are all assumed equal to l. Z_{S1} and Z_{S2} can be written as follows:

$$\frac{Z_{S1}}{Z_0} = j\frac{Z_2}{Z_0}\cdot\frac{Z_2\tan^2(\theta)-Z_1}{(Z_2+Z_1)\tan(\theta)} \tag{3}$$

$$\frac{Z_{S2}}{Z_0} = j\frac{Z_4}{Z_0}\cdot\frac{Z_4\tan^2(\theta)-Z_3}{(Z_4+Z_3)\tan(\theta)} \tag{4}$$

where θ is the electrical length of each section line of the DBR

$$\theta = \frac{2\pi\cdot F}{c_0}l. \tag{5}$$

F, c_0, and Z_0 are the frequency, the speed of light in vacuum, and the reference impedance, respectively.

One of these equivalent input impedances has to be set to zero (parallel short circuit conditions) to obtain a transmission zero. This leads to the following equations:

$$\tan^2(\theta_1) = \frac{Z_1}{Z_2} \tag{6}$$

$$\tan^2(\theta_2) = \frac{Z_3}{Z_4} \tag{7}$$

where

$$\theta_1 = \frac{2\pi k_1 F_0}{c_0}l \tag{8}$$

$$\theta_2 = \frac{2\pi k_2 F_0}{c_0}l \tag{9}$$

and F_0, k_1F_0, and k_2F_0 are the central frequency and the frequencies of the first and second transmission zeros, respectively.

Then, the condition of constructive recombination has to be simultaneously recovered at F_o as

$$Z_{S1} + Z_{S2} = 0. \tag{10}$$

So, the electrical length of each section can be expressed according to its characteristic impedances at F_0

$$\tan^2(\theta_0) = \frac{Z_1Z_2(Z_3+Z_4)+Z_3Z_4(Z_1+Z_2)}{Z_2^2(Z_3+Z_4)+Z_4^2(Z_1+Z_2)}. \tag{11}$$

Finally, the bandwidth around F_o can be determined by calculating the slope parameter of the DBR structure. This is achieved by deriving the susceptance $B(\omega)$

$$b = \frac{\omega_0}{2}\left.\frac{\partial B(\omega)}{\partial\omega}\right|_{\omega_0} \tag{12}$$

where ω is the pulsation and ω_0 is the central pulsation corresponding to F_0.

As the total admittance of the DBR is defined by

$$\frac{Y}{Y_0} = Z_0\left(\frac{Z_{s1}+Z_{s2}}{Z_{s1}Z_{s2}}\right) \tag{13}$$

we can express $B(\omega)$ and $\partial B(\omega)/\partial\omega$ with the following equations:

$$B(\omega) = \mathrm{Im}\left\{\frac{Y}{Y_0}\right\} = \frac{P(\omega)}{Q(\omega)} \tag{14}$$

$$\left.\frac{\partial B(\omega)}{\partial\omega}\right|_{\omega_0} = \frac{P'(\omega_0)Q(\omega_0)-P(\omega_0)Q'(\omega_0)}{Q^2(\omega_0)} \tag{15}$$

according to (10) at the frequency F_o we obtain

$$P(\omega_0) = 0 \tag{16}$$

and consequently

$$\left.\frac{\partial B(\omega)}{\partial\omega}\right|_{\omega_0} = \frac{P'(\omega_0)}{Q(\omega_0)}. \tag{17}$$

In this equation $P'(\omega_0)$ and $Q(\omega_0)$ are expressed by

$$P'(\omega_0) = \frac{Z_0 l}{c_0}\left(1+\tan^2(\theta_0)\right)[R+S(\omega_0)] \tag{18}$$

and

$$Q(\omega_0) = -Z_2Z_4\frac{Z_2\tan^2(\theta_0)-Z_1}{(Z_2+Z_1)\tan(\theta_0)}\cdot\frac{Z_4\tan^2(\theta_0)-Z_3}{(Z_4+Z_3)\tan(\theta_0)} \tag{19}$$

where

$$R = \frac{Z_2^2}{(Z_2+Z_1)} + \frac{Z_4^2}{(Z_4+Z_3)} \tag{20}$$

$$S(\omega_0) = \frac{1}{\tan^2(\theta_0)}\left[\frac{Z_2Z_1}{(Z_2+Z_1)} + \frac{Z_4Z_3}{(Z_4+Z_3)}\right]. \tag{21}$$

Despite the simplifications already adopted (reference length l for all sections), the analytical equations remain complex and are not really convenient for direct synthesis. New hypotheses are, therefore, necessary in order to obtain convenient and flexible synthesis formulas.

B. Accessing to Simplified Design Equations

Several simplifications are possible according to the topology of the DBR and to its numerous parameters.

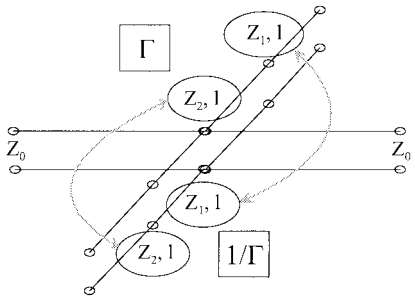

Fig. 7. Simplified DBR. $\Gamma' = 1/\Gamma$.

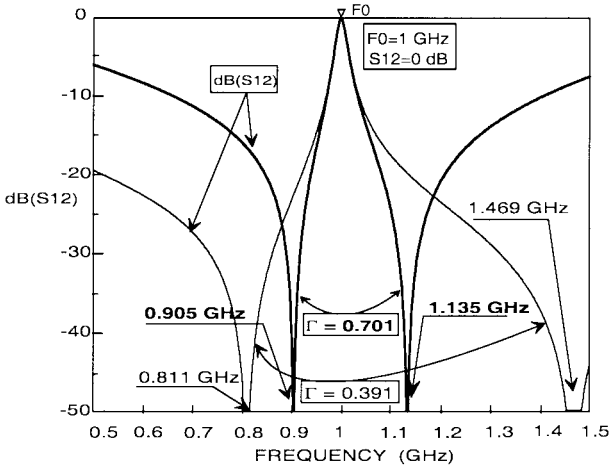

Fig. 8. Frequency responses of two simplified DBR. $\Gamma = 0.701$ and $\Gamma = 0.391$.

1) Assumption and Proposed Solution: For one DBR structure, the transmission zero frequencies depend upon the Γ, Γ' ratios as previously explained. An intuitive simplification involves identifying Γ and Γ', assuming

$$\Gamma' = \frac{1}{\Gamma}. \tag{22}$$

Consequently, two parallel stubs constituting one DBR use identical characteristic impedance values, with a geometrical inversion with respect to the Tee-junction with the input–output feeding line. This is illustrated in Fig. 7. This leads to the following relations between characteristic impedances: $Z_4 = Z_1$ and $Z_3 = Z_2$ that greatly simplify (18)–(21). On the other hand, such a simplification has some incidence on the synthesis flexibility as the equation system becomes underdetermined. If the central frequency and the associated bandwidth remain independent (fundamental filter requirements), the lower and upper transmission zeros become frequency-dependent (see Fig. 8).

Consequently, the two attenuated bands on each side of the bandpass cannot be defined and imposed independently.

2) Simplified DBR: Design Equations: According to (6) and (7) for a simplified elementary DBR, the equations relative to the transmission zeros are defined as follows:

$$Z_2 \tan^2(\theta_1) = Z_1 \tag{23}$$

$$Z_1 \tan^2(\theta_2) = Z_2. \tag{24}$$

The length l of the section lines can be derived with respect to the following parameters F_0, k_1, and k_2 as

$$l = \frac{c_0}{4F_0(k_1 + k_2)}. \tag{25}$$

Equation (11) can be summarized as

$$\tan^2(\theta_0) = \frac{2Z_1 Z_2}{Z_2^2 + Z_1^2}. \tag{26}$$

The transmission zero dependence can be expressed as a relation between k_2 and k_1. The combination of (23) to (26) leads to the relation

$$\cos\left(\frac{\pi\delta}{2\sigma}\right) = \sqrt{2}\sin\left(\frac{\pi}{2\sigma}\right) \tag{27}$$

where

$$\delta = k_2 - k_1 \tag{28}$$

and

$$\sigma = k_1 + k_2. \tag{29}$$

One can choose or impose a given value for the sum σ, and then calculate the difference value δ via (27) which leads to

$$\delta = \frac{2\sigma}{\pi} Arc\cos\left(\sqrt{2}\sin\left(\frac{\pi}{2\sigma}\right)\right). \tag{30}$$

Then, once δ and σ have been defined, parameters k_1 and k_2 are easily determined.

k_1 and k_2 being now well-defined, the impedances Z_1 and Z_2 can also be determined. By using (23) and (26), $\tan^2\theta_0$ can be expressed as follows:

$$\tan^2(\theta_0) = \frac{2\tan^2\theta_1}{1 + \tan^4\theta_1}. \tag{31}$$

By substituting (23) and (31) into (18)–(21), $P'(\omega_0)$ and $Q(\omega_0)$ become

$$P'(\omega_0) = Z_0 \frac{l}{c_0} 2.Z_2\left[1 + \tan^2\theta_1\right] \tag{32}$$

$$Q(\omega_0) = \frac{Z_2^2}{2}\tan^2\theta_1 \frac{\left(1 - \tan^2\theta_1\right)^2}{1 + \tan^4\theta_1}. \tag{33}$$

By using (12) which defines the slope parameter b, the impedance Z_2 can be expressed as follows:

$$\frac{Z_2}{Z_0} = \frac{\left(\tan^2\theta_1 + 1\right)\left(\tan^4\theta_1 + 1\right)\pi}{\tan^2\theta_1\left(1 - \tan^2\theta_1\right)^2(k_1 + k_2)b}. \tag{34}$$

3) Filter: Design Equations: These DBRs can now be modeled by their equivalent slope parameter b. A classical formalism can be used to synthesize an nth-order filter [31]. The resonators being defined by a proper b_j coefficient, the designer has just to calculate the characteristic impedances $Z_{cj,j+1}$ of the quarter wavelength admittance inverters defined as follows:

$$\frac{Z_{Cj,j+1}}{Z_0} = \frac{1}{J_{j,j+1}} \tag{35}$$

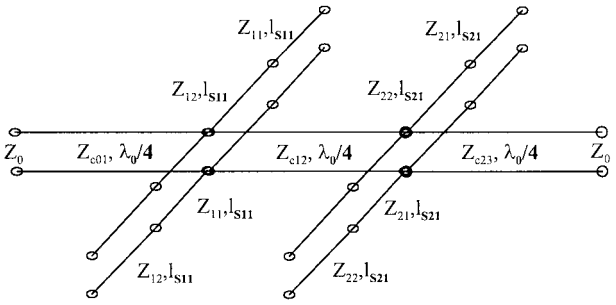

Fig. 9. Ideal transmission-line scheme used for simulation.

where

$$J_{01} = \sqrt{\frac{G_a \cdot b_1 \cdot w}{w_1' \cdot g_0 \cdot g_1}} \tag{36}$$

$$J_{j,j+1} = \frac{w}{w_1}\sqrt{\frac{b_j \cdot b_{j+1}}{g_j \cdot g_{j+1}}} \tag{37}$$

$$J_{n,n+1} = \sqrt{\frac{G_b \cdot b_n \cdot w}{w_1' \cdot g_n \cdot g_{n+1}}}. \tag{38}$$

In these formulas, the coefficients g_j are the Tchebyscheff coefficients of the equivalent low-pass filter prototype and define the bandwidth ondulation. The parameters w_1' is the cut-off frequency of the low-pass prototype and G_a and G_b are the terminating conductances of the circuit. Finally, w is defined as the fractional bandwidth.

As we use an admittance inverter, the b_j coefficients can be used as a dimensionless constant. In this way, a tuning parameter is thus introduced. This parameter can be chosen arbitrarily, mostly depending on the achievable characteristic impedance values of the technology in use.

The synthesis development is now complete and can be employed to design an nth-order filter with two frequency-dependent attenuated bands presenting $2n$ transmission zeros.

IV. Second-Order Filter Theoretical Responses

In this section, we discuss the numerous possibilities of this new class of bandpass filter via several examples. A second-order filter ($F_0 = 4$ GHz) is synthesized, with a 0.01-dB ripple and a 4% relative bandwidth. By modifying the values of the transmission zero frequencies, successive comparisons are proposed to highlight the great flexibility of the suggested design. Ideal transmission lines are considered for the filter scheme (see Fig. 9), neglecting losses and discontinuity effects.

For each simulation, the different electrical parameters of the filter (characteristic impedances, inverters, and resonators lengths) are presented with the associated electrical response. The particular frequency parameters k_{i1} and k_{i2} associated with each ith DBR are also given.

A. Symmetric Filter

The first simulation shows the electrical response of a symmetric filter. Indeed, the transmission zeros implied by DBRs 1 and 2 appear at the same lower and upper frequencies:

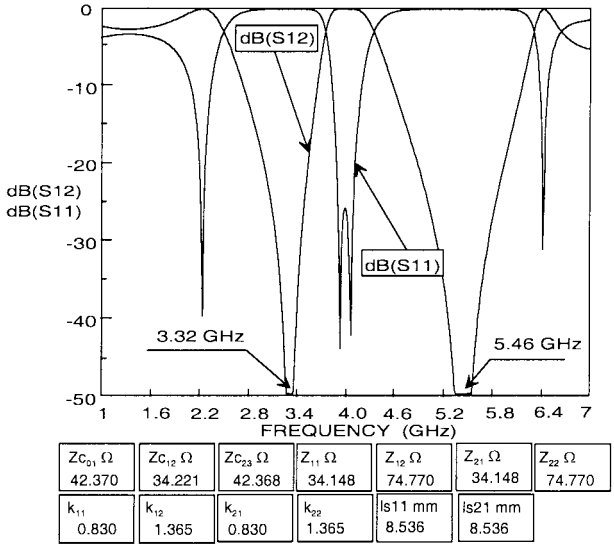

Fig. 10. Electrical response of a second-order symmetric filter.

$k_{11}F_0 = k_{21}F_0 = 0.83F_0 = 3.32$ GHz for the lower transmission zeros and $k_{12}F_0 = k_{22}F_0 = 1.365F_0 = 5.46$ GHz for the upper transmission zeros. The electrical response is presented in Fig. 10.

This kind of "symmetric" filter contributes to improving the out-of-band rejection levels (double transmission zero at discrete frequencies). As a comparison, a third-order filter based upon classical topologies would have been required to obtain an equivalent rejection level. Asymmetric solutions allow the control of attenuated frequency bands by properly separating the transmission zeros.

B. Asymmetric Filters

The location of the transmission zeros can be gradually modified and thus allows one to control the width of the attenuated bands while maintaining the desired operating bandwidth. Two examples are presented below.

Only the second DBR is modified at first (Fig. 11) with respect to the previous symmetric configuration. Its transmission zeros are chosen as follows:

$$k_{21}F_0 = 0.867F_0 = 3.47 \text{ GHz (lower transmission zero)}$$
$$k_{22}F_0 = 1.228F_0 = 4.91 \text{ GHz (lower transmission zero)}.$$

As expected, two double transmission zeros appear within the two attenuated frequency bands. Additional transmission zeros can be considered by either similarly modifying the first DBR conditions or increasing the order of the filter.

The width of the rejected bands can be also broadened by spacing the transmission zeros' location by choosing higher values for the δ parameters of each DBR. In the following example (see Fig. 12), the attenuated bandwidth is extended in this way. The frequency parameters are defined as follows:

$$\text{1st DBR}: k_{11}F_0 = 0.781F_0 = 3.12 \text{ GHz}$$
$$k_{12}F_0 = 1.714F_0 = 6.85 \text{ GHz}.$$
$$\text{2nd DBR}: k_{21}F_0 = 0.83F_0 = 3.32 \text{ GHz}$$
$$k_{22}F_0 = 1.385F_0 = 5.46 \text{ GHz}.$$

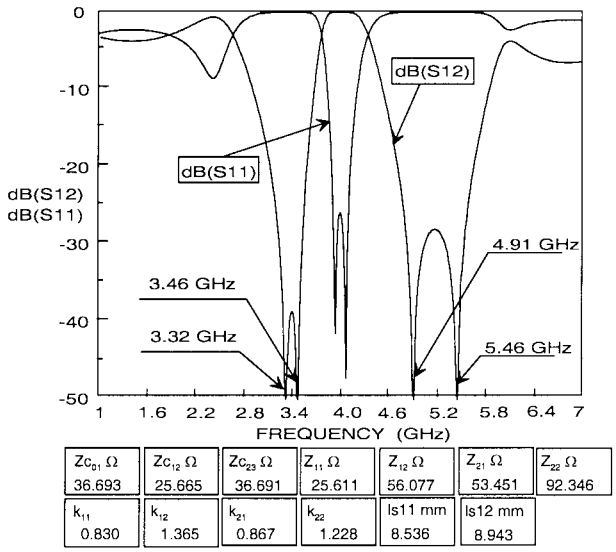

Fig. 11. Electrical response of a second-order asymmetric filter.

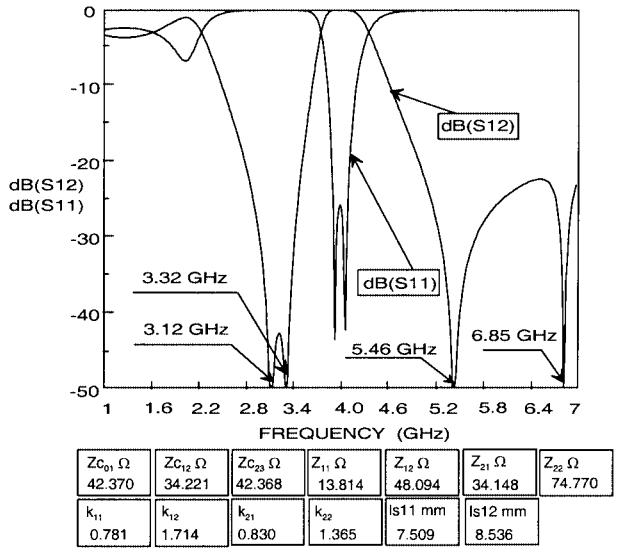

Fig. 12. Electrical response of a second-order asymmetric filter.

The associated response is presented in Fig. 12 and shows wider attenuated frequency bands compared to the previous case.

As shown in these three examples, for a given central operating bandwidth the proposed synthesis allows independent control of the attenuated bands. However, as the zeros of each single resonator are frequency-dependent further to design simplifications, the attenuated bands are dependent as well. This also results in weak dynamics on the tunable frequency range of the lower attenuated band. Therefore, compromises may sometimes be chosen in order to improve one rejected frequency band with respect to the other one.

V. Experimental Results

In order to validate the design principles stated previously, two microstrip filters were designed on a classical substrate (thickness $h = 635\ \mu$m, relative permittivity $\varepsilon_r = 10$, and $\tan\delta = 2.10^{-3}$). They were defined with equivalent relative bandwidth (4%) and central frequency (4 GHz). This relatively low frequency F_o was chosen to minimize discontinuity effects (parasitic influence and CAD model accuracy). The filters were designed using a circuit simulator (Agilent ADS) based upon conventional transmission-line description and standard discontinuity models. Metallic and dielectric losses were taken into account in the simulation.

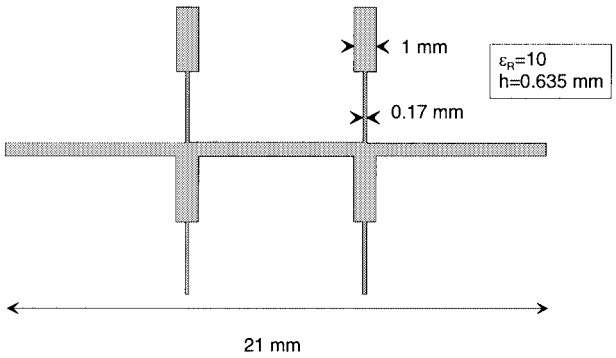

Fig. 13. Layout of a second-order microstrip filter.

Fig. 13 gives the layout of a second-order filter. As this filter is symmetrical, its theoretical electrical response presents two double zeros at 3.37 and 5.66 GHz.

Theoretical and experimental responses are presented in Fig. 14. They show correct agreement over the measured frequency range. The experimental central frequency and the two transmission zeros appear at 3.73, 3.2, and 5.55 GHz, respectively. The discrepancy between the two responses can be attributed to several factors: 1) the lack of accuracy of asymmetric cross junction discontinuity models and 2) the strong dispersion of the effective characteristics of the substrate (epsilon value and thickness).

The layout presented in Fig. 15 shows a fifth-order filter, which is nonsymmetric in terms of transmission zeros. It, therefore, induces two double transmission zeros at 4.57 and 5.14 GHz and a single transmission zero at 4.9 GHz. The corresponding zeros in the low-frequency region are located around 3.4 GHz.

Theoretical and experimental responses are presented in Fig. 16. Good agreement is observed over a wide frequency range from 1 to 8 GHz. Rejections of about -150 and -45 dB are reached in theory and experimentally, respectively. Like in the previous example, the difference between the two responses results from the same factors. In this case, the frequency shift is less important because the dispersion of the effective characteristics of the substrate (epsilon value and thickness) is lower than in the previous case.

VI. Strong and Weak Points

The special feature of this topology is its use of the constructive recombination induced by two different shunt stubs as a real bandpass. This fact implies certain advantages in comparison with classical topologies.

One of the main distinctive features of this kind of filter is that it presents a narrow bandpass by using stubs instead of coupled lines. Indeed, as this bandpass is induced by a constructive recombination between two transmission zeros,

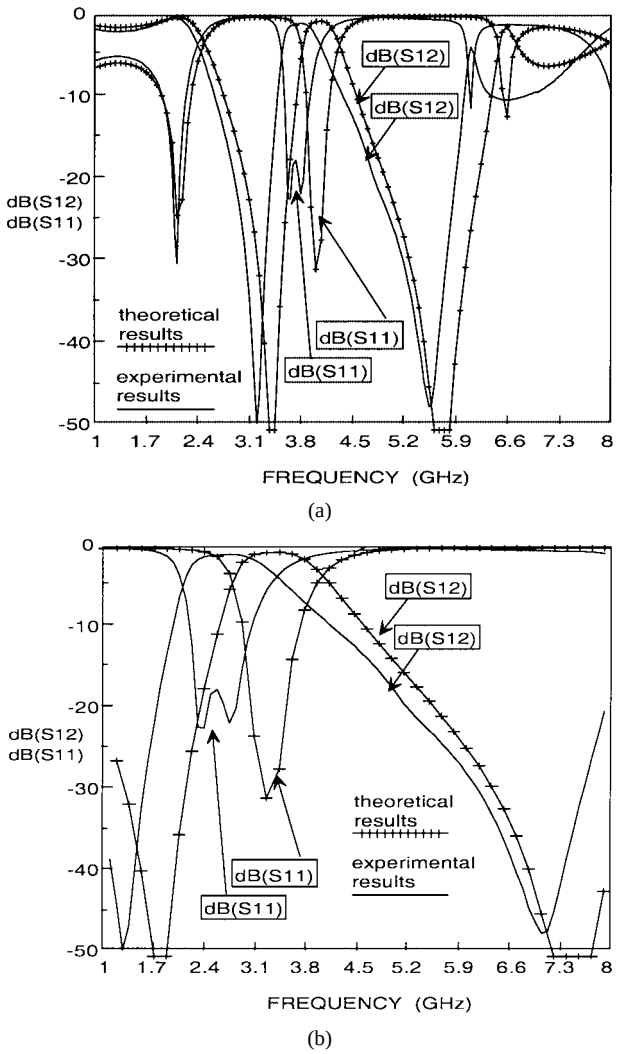

Fig. 14. Experimental and simulated electrical response of the second-order microstrip filter. (a) Broad-band frequency response. (b) Zoom-in for narrow-band characteristics.

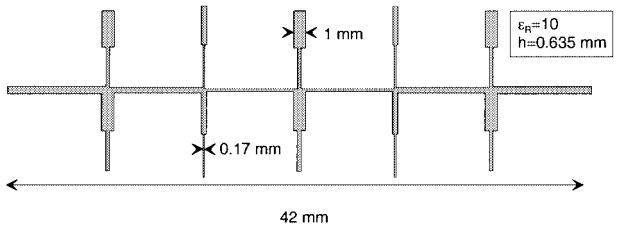

Fig. 15. Layout of a fifth-order microstrip filter.

the fractional bandwidth is very narrow. For example, by both using a classical alumina substrate (thickness $h = 635$ or 254 μm, relative permittivity $\varepsilon_r = 10$, $\tan\delta = 2.10^{-3}$) and considering a microstrip implementation, filters that present a fractional bandwidth of about a few percent up to 20% are achievable. Therefore, seeing that the DBR filters have the same achievable fractional bandwidth as coupled line filters, the two solutions need comparison.

The first strong point of this topology is obviously the possibility of placing transmission zeros at prescribed frequencies. Indeed, these transmission zeros lead to a reduction of the filter order by considering a fixed rejection and so reduce the losses of the whole structure. Compared to the traditional coupled line topology, significant improvements are noted. In particular, it allows one to control both the bandwidth and the width of the attenuated bands.

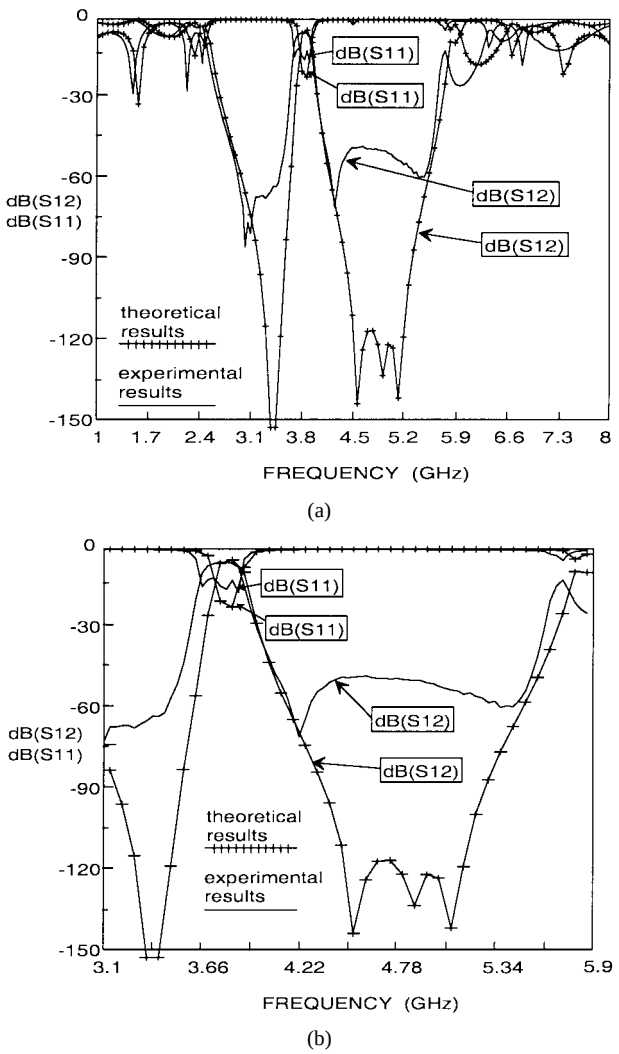

Fig. 16. Experimental and simulated electrical response of the fifth-order microstrip filter. (a) Broad-band frequency response. (b) Zoom-in for narrow-band characteristics.

The second advantage concerns the problems of packaging. Indeed, as no coupling phenomenon is used to synthesize the DBR filters, the influence of metallic cover is very low.

In this paper, we presented a specific example with stepped impedance stubs, but other solutions leading to different frequency responses can also be studied. For instance, according to the nature of the stubs, one can improve the rejection on only one side of the bandpass or obtain symmetrical attenuated bands on each side of the bandpass.

However, this structure displays an important weak point. Indeed, by considering that the constructive recombination is placed between the intrinsic resonance of each different stub, the spurious resonances are closer to the bandpass than coupled line filters. One way to control this spurious resonance involves integrating a low-pass [32] and a high-pass structure in each element of the filter while keeping its global size.

VII. Conclusion

This paper reports on a new class of filter based on DBRs. The frequency response of such a resonator is comparable to that of a first-order filter with an additional transmission zero on each side of the central bandwidth. The use of these resonators significantly increases the out-of-band rejection once the transmission zeros have been properly placed to create and control the width of two attenuated bands. A global synthesis was written and simplification procedures proposed so as to easily extract fundamental filter parameters and dimensions. The design principles as well as the DBR performances have been discussed and validated through theoretical and experimental comparisons.

Some additional effort needs to be made in order to take into account possible parasitic coupling between adjacent DBRs. If this point is not a problem, here, according to the electrical specification of the chosen filter and of the dielectric substrate characteristics, i.e., thickness and dielectric constant, it can become very important in other cases. Consequently, it should not be neglected and we are presently working on it.

Our second aim is to define a new DBR together with the associated synthesis that would lead to a complete independence of the two transmission zeros and pole.

References

[1] I. Hunter, *Theory and Design of Microwave Filters*. London, U.K.: IEE Press, 2000, pp. 3–6.

[2] S. J. Fiedziuszko, J. A. Curtis, S. C. Holme, and R. S. Kwok, "Low loss multiplexers with planar dual mode HTS resonators," *IEEE Trans. Microwave Theory Tech.*, vol. 44, pp. 1248–1257, July 1996.

[3] R. Mansour, S. Ye, V. Dokas, B. Jolley, G. Thomson, W.-C. Tang, and C. M. Kudsia, "Design consideration of superconductive input multiplexers for satellite applications," *IEEE Trans. Microwave Theory Tech.*, vol. 44, pp. 1213–1228, July 1996.

[4] A. E. Atia and A. E. Williams, "Narrow-bandpass waveguide filters," *IEEE Trans. Microwave Theory Tech.*, vol. MTT-20, pp. 258–265, Apr. 1972.

[5] L. Accatino, G. Bertin, and M. Mongiardo, "An elliptic cavity for triple mode filters," in *IEEE MTT-S Int. Microwave Symp. Dig.*, Anaheim, CA, June 1999, pp. 1037–1040.

[6] T. Hiratsuka, T. Sonoda, and S. Mikami, "A Ka-band diplexer using planar TE mode dielectric resonators with plastic package," in *Proc. Eur. Microwave Conf.*, Munich, Germany, 1999, pp. 99–102.

[7] M Mattes, J. Mosig, and M. Guglielmi, "Six-pole triple mode filters in rectangular waveguide," in *IEEE MTT-S Int. Microwave Symp. Dig.*, Boston, MA, June 2000, pp. 1775–1778.

[8] S. J. Fiedziusko, "Dual mode dielectric resonator loaded cavity filters," *IEEE Trans. Microwave Theory Tech.*, vol. MTT-30, pp. 1311–1316, Sept. 1982.

[9] F. A. Zaki, C. Chen, and A. E. Atia, "Dual mode dielectric resonator filters without iris," in *IEEE MTT-S Int. Microwave Symp. Dig.*, June 1987, pp. 141–144.

[10] Y. Ishikawa, T. Hiratsuka, S. Yamashita, and K. Iio, "Planar type dielectric resonator filter at millimeter-wave frequency," *IEICE Trans. Electron.*, vol. E79-C, no. 5, pp. 679–684, May 1996.

[11] J.-S. Hong and M. J. Lancaster, "Back-to-back open loop resonator filters with aperture couplings," in *IEEE MTT-S Int. Microwave Symp. Dig.*, Anaheim, CA, June 1999, pp. 1239–1242.

[12] J.-T. Kuo, M.-J. Maa, and P.-H. Lu, "A microstrip elliptic function filter with compact miniaturized hairpin resonators," *IEEE Microwave Guided Wave Lett.*, vol. 10, pp. 94–95, Mar. 2000.

[13] H. Yabuki, M. Sagawa, M. Matsuo, and M. Makimoto, "Stripline dual-mode ring resonators and their application to microwave devices," *IEEE Trans. Microwave Theory Tech.*, vol. 44, pp. 723–729, May 1996.

[14] M. C. Horton and R. J. Wenzel, "The digital elliptic filter—A compact sharp-cutoff design for wide bandstop or bandpass requirements," *IEEE Trans. Microwave Theory Tech.*, vol. MTT-15, pp. 307–314, May 1967.

[15] B. M. Schiffman, "A multiharmonic rejection filter designed by an exact method," *IEEE Trans. Microwave Theory Tech.*, vol. MTT-12, pp. 512–516, Sept. 1964.

[16] R. Levy and I. Whiteley, "Synthesis of distributed elliptic-function filters from lumped constant prototypes," *IEEE Trans. Microwave Theory Tech.*, vol. MTT-14, pp. 506–517, Nov. 1966.

[17] J. D. Rhodes, "The stepped digital elliptic filter," *IEEE Trans. Microwave Theory Tech.*, vol. MTT-17, pp. 178–184, Apr. 1969.

[18] I. Rubinstein, R. L. Sleven, and A. F. Hinte, "Narrow-bandwidth elliptic-function filters," *IEEE Trans. Microwave Theory Tech.*, vol. MTT-17, pp. 1108–1115, Dec. 1969.

[19] B. J. Minnis, "Classes of sub-miniature microwave printed circuit filters with arbitrary passband and stopband widths," *IEEE Trans. Microwave Theory Tech.*, vol. MTT-30, pp. 1893–1900, Nov. 1982.

[20] J.-T. Tsai and C.-L. Huang, "Bandpass filters with multiple attenuation poles in the stopband," *IEICE Trans. Electron.*, vol. E83-C, no. 7, July 2000.

[21] M. H. Capstick, "Microstrip lowpass-bandpass diplexer topology," *Electron. Lett.*, vol. 35, no. 22, pp. 1958–1959, Oct 1999.

[22] J. A. G. Malherbe, "TEM pseudoelliptic-function bandstop filters using noncommensurate lines," *IEEE Trans. Microwave Theory Tech.*, vol. MTT-24, pp. 242–248, May 1976.

[23] H. C. Bell, "Narrow bandstop filters," *IEEE Trans. Microwave Theory Tech.*, vol. 39, pp. 2188–2191, Dec. 1991.

[24] H. B. Clark, "Single-passband, single stop-band narrowband filters," in *IEEE MTT-S Int. Microwave Symp. Dig.*, Boston, MA, June 2000, pp. 1657–1660.

[25] M. Salerno, R. Sorrentino, and F. Giannini, "Image parameter design of noncommensurate distributed structures: An application to microstrip low-pass filters," *IEEE Trans. Microwave Theory Tech.*, vol. MTT-34, pp. 58–65, Jan. 1986.

[26] C. Quendo, C. Person, E. Rius, and M. Ney, "Optimal design of low-pass filters using open stubs to control out-of-band," in *Proc. Eur. Microwave Conf.*, Paris, France, Oct. 2000, pp. 336–339.

[27] G. Machiarella and A. Bovatti, "Single-sided filters in microstrip technology," in *Proc. Eur. Microwave Conf.*, London, U.K., Sept. 2001, pp. 45–48.

[28] K. Wada and I. Awai, "Design of a bandpass filter with multiple attenuation poles based on tapped resonators," *IEICE Trans. Electron.*, vol. E82-C, no. 7, pp. 1116–1122, July 1999.

[29] K. Wada and O. Hashimoto, "Fundamentals of open-ended resonators and their application to microwave filters," *IEICE Trans. Electron.*, vol. E83-C, no. 11, pp. 1763–1775, Nov. 2000.

[30] C. Quendo, E. Rius, and C. Person, "Nouvelle topologie de filtre planaire à bande étroite et à zéro de transmission utilisant des stubs à saut d'impédance" (in France), *J. Nat. Micro-ondes*, pp. 60–61, May 2001.

[31] G. L. Matthaei, L. Young, and E. M. T. Jones, *Microwave Filters, Impedance-Matching Networks, and Coupling Structures*. Norwell, MA: Artech House, 1980, pp. 427–433.

[32] C. Quendo, E. Rius, C. Person, and M. Ney, "Integration of optimized low-pass filters in a bandpass filter for out-of-band improvement," *IEEE Trans. Microwave Theory Tech.*, vol. 49, pp. 2376–2383, Dec. 2001.

Cedric Quendo was born in Plouay, France, on September 15, 1974. He received the Ph.D. degree in electronics from the University of Brest, Brest, France, in 2001.

He currently conducts research with the Laboratoire d'Electronique et Systèmes de Télécommunication (LEST), University of Brest. His research activities principally concern the modelization and design of microwave passive devices for microwave and millimeter-wave applications.

Eric Rius was born in Auray, France, on March 6, 1966. He received the Ph.D. degree in electronics from the University of Brest, Brest, France, in 1994.

Since 1995, he has been an Assistant Professor with the Electronic Department, Université de Bretagne Occidentale, Brest, France, where he currently conducts research with the Laboratory of Electronics and Communications systems (LEST). His research activities principally concern the design of filters and associated RF modules for microwave and millimeter-wave applications.

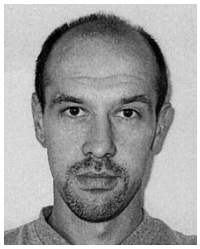

Christian Person received the Ph.D. degree in electronics from the University of Brest, Brest, France in 1994.

Since 1991, he has been an Assistant Professor with the Microwave Department, Ecole Nationale Supérieure des Télécommunications de Bretagne, Brest, France, where he currently conducts research with the Laboratoire d'Electronique et Systèmes de Télécommunication (LEST). His research concerns the development of new technologies for millimeter-wave applications and systems. His research activities are especially focused on hybrid three-dimensional (3-D) integration techniques for implementing optimized passives functions (filters, antennas, couplers) and improving reliability and interconnection facilities with active monolithic microwave integrated circuits (MMICs). He is also involved in the design of reconfigurable structures by means of microelectromechanical systems (MEMs) or active hybrid circuits for smart antennas and software radio RF equipments.